

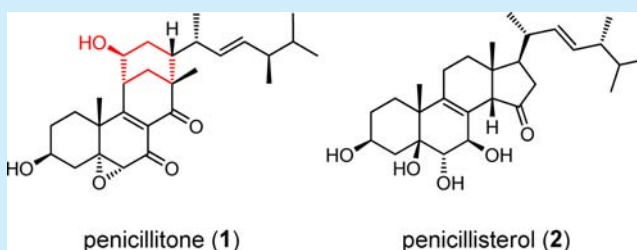
# Penicillitone, a Potent *in Vitro* Anti-inflammatory and Cytotoxic Rearranged Sterol with an Unusual Tetracycle Core Produced by *Penicillium purpurogenum*

Jinghua Xue,<sup>†</sup> Ping Wu,<sup>†</sup> Liangxiong Xu, and Xiaoyi Wei\*

Key Laboratory of Plant Resources Conservation and Sustainable Utilization, South China Botanical Garden, Chinese Academy of Sciences, Xingke Road 723, Tianhe District, Guangzhou 510650, People's Republic of China

## S Supporting Information

**ABSTRACT:** A rearranged sterol with an unusual tetracycle core skeleton, penicillitone (1), and a new sterol, penicillisterol (2), were obtained from the culture of the fungus *Penicillium purpurogenum* SC0070. Their structures were characterized by spectroscopic analysis, DFT/TDDFT computations, and X-ray diffraction. Compound 1 demonstrated potent inhibitory effects on tumor cell growth and key pro-inflammatory cytokine production in macrophages. A biogenetic pathway with oxidative cleavage and vinylogous aldol addition as key reactions is proposed for 1.



Sterols are of the most important small molecules in biology, as they are constituents of the plasma membrane of eukaryotes and play multiple cellular roles associated with membrane structural and signaling functions.<sup>1,2</sup> Their derivatives include dozens of physiologically active endogenous substances, such as steroid hormones in vertebrates, ecdysteroids in insects, and brassinosteroids in plants, which participate in the control of cell proliferation and tissue differentiation and regulation of signal transductions.<sup>3,4</sup> Sterol-derived drugs, representing the second largest drug category and being among the most marketed medical products, are of great importance for improvement of life quality and prevention and therapy of diseases.<sup>5</sup> Therefore, sterols and their derivatives attract the continual renewal of attention from chemists and biologists.<sup>1</sup> During a screening for antibacterial natural products produced by the fungi collected in South China, the mycelial solid culture extract of the strain *Penicillium purpurogenum* SC0070 was found to be active against *Staphylococcus aureus*. The secondary metabolites of this fungus were therefore investigated, and two new sterol derivatives (Figure 1), penicillitone (1) and penicillisterol (2), were obtained, of which 1 had an unusual tetracycle core skeleton and exhibited

potent tumor cell growth inhibitory and *in vitro* anti-inflammatory activities. Herein, we report the isolation, structure elucidation, and bioactivities of these compounds. The plausible biogenetic pathway of 1 from ergosterol with oxidative cleavage and vinylogous aldol addition as key reactions is also described.

The EtOH extract of the solid culture of *P. purpurogenum* SC0070 fermented on cooked wheat was partitioned by successive extraction with  $\text{CHCl}_3$ , EtOAc, and *n*-BuOH. The  $\text{CHCl}_3$ -soluble fraction was separated by repeated column chromatography over silica gel, ODS, Sephadex LH-20, and HPLC or preparative TLC to yield new compounds 1 and 2.

Penicillitone (1), obtained as colorless cubes, mp 240–242 °C (EtOAc),  $[\alpha]_{\text{D}}^{20} +102.9$  (*c* 0.55, MeOH), was determined to have the molecular formula  $\text{C}_{28}\text{H}_{40}\text{O}_5$  from the HR-ESI(+)MS ion at  $m/z$  457.2952  $[\text{M} + \text{H}]^+$  (calcd:  $m/z$  457.2949). The  $^1\text{H}$  and  $^{13}\text{C}$  NMR spectra (Table 1) in combination with the HSQC spectrum showed the presence of six methyls ( $\delta_{\text{H}}$  0.78, 0.80, 0.85, 1.01, 1.16, and 1.28;  $\delta_{\text{C}}$  20.1, 20.5, 18.2, 22.6, 23.7, and 22.8), ten methines including three oxymethines ( $\delta_{\text{H}}$  4.21, 3.82, and 3.35;  $\delta_{\text{C}}$  66.2, 68.4, and 63.7) and two olefinic methines constituting a *trans*-1,2-disubstituted olefin ( $\delta_{\text{H}}$  5.07 and 5.04;  $\delta_{\text{C}}$  135.2 and 132.6), five methylenes, and seven quaternary carbons, of which two were conjugated ketone carbonyls ( $\delta_{\text{C}}$  198.2 and 193.3), two were olefinic ( $\delta_{\text{C}}$  176.0 and 130.7), and one was oxygenated ( $\delta_{\text{C}}$  65.2). Analysis of the  $^1\text{H}$ – $^1\text{H}$  COSY spectrum identified two structural fragments, one from C-1 to C-4 and the other from C-12 via C-11 to C-28 (Figure 2). In the HMBC spectrum, key correlations (Figure 2) were observed from  $\text{H}_3$ -19 to C-1, C-5,

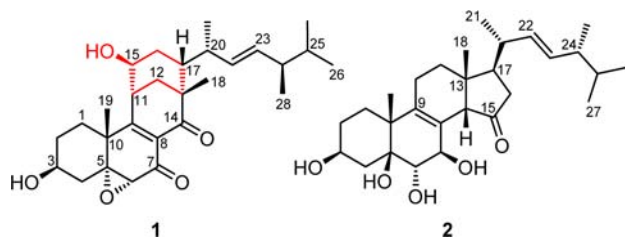


Figure 1. Structures of 1 and 2.

Received: February 10, 2014

Published: February 27, 2014

Table 1.  $^1\text{H}$  (600 MHz) and  $^{13}\text{C}$  (150 MHz) NMR Data of **1** and **2**

position	1 (in acetone- $d_6$ )		2 (in $\text{C}_5\text{D}_5\text{N}$ )	
	$\delta_{\text{H}}$ (multi, $J$ in Hz)	$\delta_{\text{C}}$	$\delta_{\text{H}}$ (multi, $J$ in Hz)	$\delta_{\text{C}}$
1	$\alpha$ 1.91 (td, 13.0, 3.4) $\beta$ 2.13 (dt, 13.0, 3.4)	29.2	$\alpha$ 1.65 (dt, 14.2, 3.1) $\beta$ 2.37 (td, 14.2, 3.1)	26.9
2	$\alpha$ 2.04 (m) $\beta$ 1.73 (m)	30.9	$\alpha$ 1.42 (m) $\beta$ 1.87 (m)	31.3
3	3.82 (m, $W_{1/2} = 23.8$ ) <sup>a</sup>	68.4	4.28 (br s, $W_{1/2} = 10.8$ ) <sup>a</sup>	67.1
4	$\alpha$ 1.53 (dd, 13.3, 2.2) $\beta$ 2.29 (dd, 13.3, 11.7)	39.1	$\alpha$ 1.98 (overlapped) $\beta$ 2.66 (m)	33.1
5		65.2		77.0
6	3.35 (s)	63.7	4.54 (d, 7.7)	76.8
7		193.3	5.05 (br d, 7.7)	74.1
8		130.7		128.7
9		176.0		136.4
10		43.6		45.1
11	2.81 (q, 2.8)	40.6	2.17 (br s, 2H)	22.0
12	$\alpha$ 2.36 (dd, 12.8, 2.8) $\beta$ 1.68 (dd, 12.8, 2.8)	39.2	$\alpha$ 1.70 (ddd, 13.4, 8.2, 6.8) $\beta$ 1.43 (m)	33.8
13		45.4		40.6
14		198.2	3.91 (s)	55.9
15	4.21 (q, 2.8)	66.2		218.5
16	$\alpha$ 1.50 (td, 13.5, 2.8) $\beta$ 1.65 (dt, 13.5, 2.8)	29.3	$\alpha$ 2.61 (dd, 19.2, 9.4) $\beta$ 2.42 (ddd, 19.2, 5.1, 1.2)	39.3
17	1.76 (m)	46.5	1.98 (overlapped)	47.2
18	1.16 (s, 3H)	23.7	1.22 (s, 3H)	20.4
19	1.28 (s, 3H)	22.8	1.38 (s, 3H)	25.1
20	2.71 (m)	34.7	2.64 (m)	38.3
21	1.01 (d, 7.0, 3H)	22.6	1.09 (d, 6.8, 3H)	22.1
22	5.04 (dd, 15.6, 6.4)	132.6	5.44 (dd, 15.3, 8.2)	132.7
23	5.07 (dd, 15.6, 6.4)	135.2	5.38 (dd, 15.3, 7.8)	135.5
24	1.76 (m)	44.2	1.78 (m)	44.1
25	1.41 (m)	33.8	1.43 (m)	33.6
26	0.80 (d, 6.8, 3H)	20.5	0.82 (d, 6.8, 3H)	20.3
27	0.78 (d, 6.8, 3H)	20.1	0.82 (d, 6.8, 3H)	20.6
28	0.85 (d, 6.8, 3H)	18.2	1.00 (d, 6.8, 3H)	18.2
OH	4.06 (d, 4.5, 3-OH)		6.69 (br s, 3-OH); 5.99 (s, 5-OH); 6.71 (br s, 7-OH)	

<sup>a</sup> $W_{1/2}$ : half-height width of the signal, in Hz.

C-9, and C-10, from H-3 to C-5, from H-6 to C-4, C-5, C-7, C-8, and C-9, from H<sub>3</sub>-18 to C-12, C-13, C-14, and C-17, from H-15 to C-9, C-12, C-16, and C-17, from H-11 to C-8 and C-9, and from H<sub>2</sub>-12 to C-9, C-13, and C-14, which indicated that C-5–C-14 constitute a hexahydronaphthalene-1,8-dione moiety and the two deduced structural fragments are connected via this bicyclic moiety, constructing a unprecedented carbon skeleton for **1**. The downfield  $^1\text{H}$  and  $^{13}\text{C}$  NMR chemical shifts of the positions C-3, C-5, C-6, and C-15, in association with the molecular formula, showed the presence of 3-OH, 15-OH, and 5,6-epoxy groups and assigned the gross structure as shown.

The relative configuration of the tetracyclic nucleus in **1** was established by analysis of the NOESY spectrum and  $^1\text{H}$  NMR coupling constants. Key NOE interactions (Figure 2) were observed for H<sub>3</sub>-19/H-1 $\beta$ , H<sub>3</sub>-19/H-4 $\beta$ , H<sub>3</sub>-19/H-11, H-3/H-1 $\alpha$ , H-3/H-4 $\alpha$ , H-6/H-4 $\alpha$ , H-11/H-1 $\alpha$ , H<sub>3</sub>-18/H<sub>2</sub>-12, H<sub>3</sub>-18/H-17, H<sub>3</sub>-18/H-20, and H-15/H-1 $\alpha$ . These observations together with the vicinal proton coupling constants,  $J_{3,4\beta} = 11.7$  Hz,  $J_{3,4\alpha} = 2.2$  Hz,  $J_{11,15} = J_{15,16\alpha} = J_{15,16\beta} = J_{16\beta,17} = 2.8$  Hz, and  $J_{16\alpha,17} = 13.5$  Hz (Table 1), indicated that 3-OH, 15-OH, and 13-CH<sub>3</sub> are all in a  $\beta$ -orientation and, at the equatorial position, the side chain at C-17 is also equatorial but in an  $\alpha$ -orientation, and 5,6-epoxy is  $\alpha$ -oriented. These findings fully

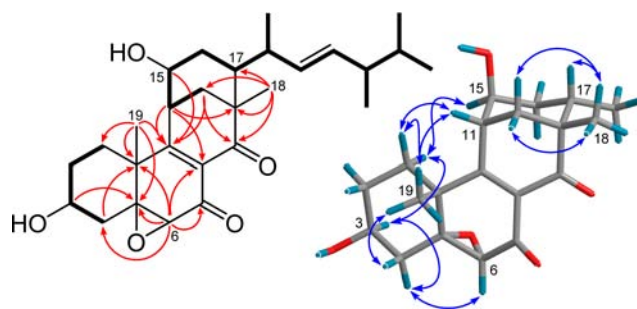


Figure 2.  $^1\text{H}$ – $^1\text{H}$  COSY (bold lines) and key HMBC (red arrows) and NOESY (blue double-headed arrows) correlations of **1**. The side chain at C-17 in the 3D-conformer is replaced by a methyl.

match up with the lowest-energy conformer (Figure 2) and other low-energy minima (3-OH and 15-OH rotamers of the lowest-energy conformer), which were generated from the truncated structure (17-side chain replaced by a methyl) of **1** by an MMFF conformational search followed by geometry optimization using the DFT method at the B3LYP/6-31G(d,p) level. Further, ECD/TDDFT calculations of the low-energy conformer afforded predicted ECD spectra consistent with the

experimental one (see Supporting Information), indicating the absolute configuration of the nucleus to be as depicted in Figure 1. Finally, a single crystal was obtained and subjected to X-ray diffraction analysis. The result (Figure 3)<sup>6</sup> confirmed the structure and determined the absolute configuration of the side chain to be 20*R*,24*R*.

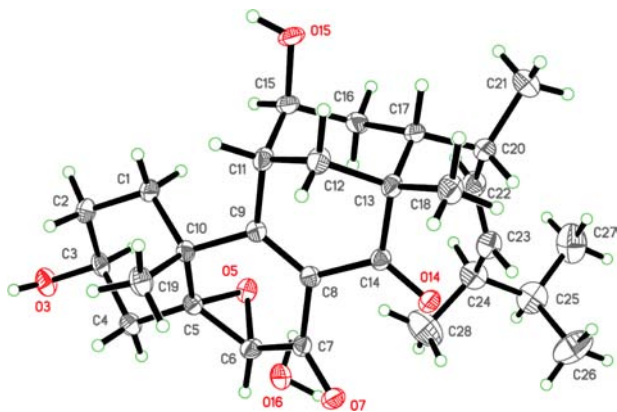
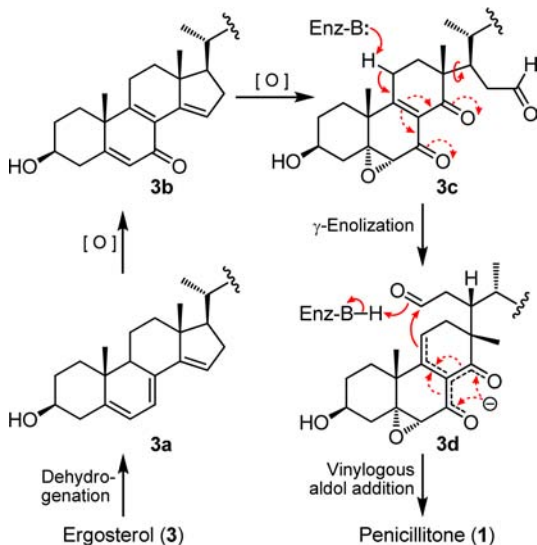


Figure 3. X-ray structure of **1**.

Compound **1** is likely derived from ergosterol (**3**) which was also obtained in the present study. The plausible biogenetic pathway is proposed as shown in Scheme 1. The biosynthesis

#### Scheme 1. Plausible Biogenetic Origin of **1**



would be initiated by dehydrogenation of **3** to afford the tetraenol **3a**,<sup>7</sup> followed by oxidation to give the tetraenone **3b**.<sup>8</sup> Further oxidation would cleave the double bond between C-14 and C-15 to generate the direct precursor **3c** which would undergo an intramolecular vinyllogous aldol reaction<sup>9,10</sup> via the dienolate **3d** to give **1**. The key step in this pathway is the oxidative cleavage that not only generates an aldehyde (C-15) function as the electrophile but also creates an additional carbonyl (C-14) at the  $\alpha$ -position (C-8) of the  $\alpha,\beta$ -unsaturated ketone moiety. The latter could increase the acidity of  $\gamma$ -hydrogens (H<sub>2</sub>-11) and therefore facilitate  $\gamma$ -enolization and enhance the validity of the aldol reaction. To the best of our knowledge, this biogenetic mechanism is so far not reported in biosynthesis and biological and chemical transformations of

sterols and it could be the first example of vinyllogous aldol reactions involved in sterol metabolism. Further, the structural profile of the nucleophile  $\alpha$ -ketone carbonyl  $\alpha,\beta$ -unsaturated ketone moiety in **3c** might provide the inspiration for the design of new vinyllogous aldol motifs to construct relevant molecules.

Penicilliterol (**2**) was obtained as a white powder,  $[\alpha]_D^{20} +19.1$  (*c* 0.18, CHCl<sub>3</sub>). Its molecular formula was determined to be C<sub>28</sub>H<sub>44</sub>O<sub>5</sub> from the quasi-molecular ion at *m/z* 483.3085 [*M* + Na]<sup>+</sup> (calcd: *m/z* 483.3081) in HR-ESIMS. The <sup>1</sup>H and <sup>13</sup>C NMR spectra (Table 1) of **2** were largely similar to those of **1**, in which resonances characteristic of the side chain in **1** were also present. Analysis of the <sup>1</sup>H–<sup>1</sup>H COSY, HSQC, and HMBC (Figure 4) assigned a gross structure of (2*E*)-3,5,6,7-

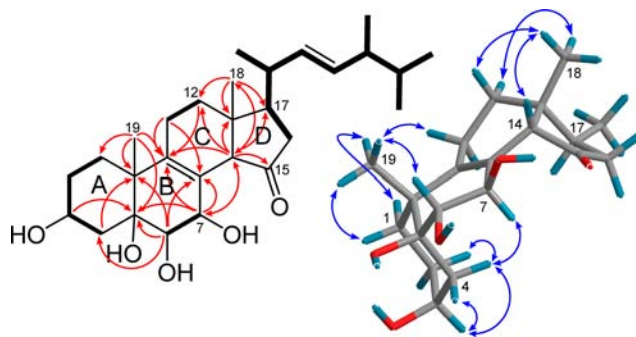


Figure 4. <sup>1</sup>H–<sup>1</sup>H COSY (bold lines) and key HMBC (red arrows) and NOESY (blue double-headed arrows) correlations of **2**. The side chain at C-17 in 3D-conformer is replaced by a methyl.

tetrahydroxyergosta-8,22-dien-15-one for **2**. The presence of key NOEs of H<sub>3</sub>-19/H-1 $\beta$ , H<sub>3</sub>-19/H-1 $\alpha$ , H<sub>3</sub>-19/H-6, H-2 $\alpha$ /H-4 $\alpha$ , H-7/H-4 $\alpha$ , and H<sub>3</sub>-18/H-14 and the absence of the NOE of H<sub>3</sub>-19/H-4 $\beta$  in the NOESY spectrum (Figure 4), in combination with the peak shape of H-3 (br s, *W*<sub>1/2</sub> = 10.8 Hz)<sup>11</sup> and the axial–axial coupling proximity of the *J*<sub>6,7</sub> value (7.7 Hz), indicated that ring A adopts a <sup>1</sup>C<sub>4</sub> conformation rather than the <sup>1</sup>C<sub>4</sub> form in **1** and 3-OH, 5-OH, 7-OH, and H-14 are all  $\beta$ -oriented while 6-OH is  $\alpha$ -oriented. This configuration was supported by conformational analysis as that for **1** as well as by ECD/TDDFT calculations which were carried out with the lowest-energy conformer (Figure 4) and provided simulated ECD spectra closely similar to the measured one (see Supporting Information). The configuration of the side chain was assigned to be the same as that of **1** by comparison of the <sup>1</sup>H and <sup>13</sup>C NMR data with those of **1** and the closely related compounds.<sup>8,12,13</sup> Thus, the structure of **2** was determined as shown, which is unusual in naturally occurring sterols due to its *cis*-ring fusion of both A/B and C/D.

Compound **2** must be also derived from **3** and share the same precursor **3a** with **1**. The subsequent oxidation of **3a** in route to **2** would, however, not break ring D but likely gives 5 $\alpha$ ,6 $\alpha$ -epoxyergosta-8(14),22-dien-3-ol 7 $\beta$ ,15 $\beta$ -peroxide as its key precursor, which would generate **1** by peroxide ring opening and a 1,3-H shift (from C-9 to C-14) (see Supporting Information). In this context, the co-occurrence of **2** with **1** could be supporting evidence for the biogenetic origin of **1**.

Compounds **1** and **2** were tested for growth inhibitory activity against A549, HepG2, and MCF-7 cells using the MTT method.<sup>14</sup> Compound **1** exhibited good potency against all the test cell lines with IC<sub>50</sub> values of 5.57 ( $\pm$ 0.19), 4.44 ( $\pm$ 0.24),

and 5.98 ( $\pm 0.22$ )  $\mu\text{M}$ , respectively, while **2** was inactive ( $\text{IC}_{50} > 100 \mu\text{M}$ ) to all these cells. Compound **1** was also evaluated for *in vitro* anti-inflammatory activity with the method already described<sup>15</sup> and demonstrated dose-dependent inhibitory effects on the production of  $\text{TNF-}\alpha$  and IL-6 in LPS-stimulated RAW 264.7 macrophages. When at 5  $\mu\text{M}$  (nontoxic to the test macrophages at this concentration), **1** was able to reduce secretion of the two pro-inflammatory cytokines by 70.7% and 96.6%, respectively. The activity was comparable to that of the steroidal anti-inflammatory drug dexamethasone at 100  $\mu\text{M}$  (inhibition rates: 87.3% and 96.7%, respectively). These findings in combination with its new carbon skeleton suggested that **1** would be promising as a new scaffold for anti-inflammatory and antitumor agents.

## ■ ASSOCIATED CONTENT

### ■ Supporting Information

Experimental section, computational details, and 1D and 2D NMR spectra and HRESIMS of **1** and **2**. These data are available free of charge via the Internet at <http://pubs.acs.org>.

## ■ AUTHOR INFORMATION

### Corresponding Author

\*E-mail: [wxy@scbg.ac.cn](mailto:wxy@scbg.ac.cn).

### Author Contributions

<sup>†</sup>These authors contributed equally.

### Notes

The authors declare no competing financial interest.

## ■ ACKNOWLEDGMENTS

We thank Prof. Xiao-Long Feng, Instrumental Analysis & Research Center, Sun Yat-sen University, for X-ray diffraction analysis and Prof. Tai-Hui Li, Guangdong Institute of Microbiology, for microbiological authentication. This work was supported by an NSFC grant (No. 81172942).

## ■ REFERENCES

- (1) Nes, W. D. *Chem. Rev.* **2011**, *111*, 6423–6451.
- (2) Dupont, S.; Lemetais, G.; Ferreira, T.; Cayot, P.; Gervais, P.; Beney, L. *Evolution* **2012**, *66*, 2961–2968.
- (3) Ikekawa, N.; Fujimoto, Y.; Ishiguro, M. *Proc. Jpn. Acad., Ser. B.* **2013**, *89*, 349–369.
- (4) Wollam, J.; Antebil, A. *Annu. Rev. Biochem.* **2011**, *80*, 885–916.
- (5) Marina, V.; Donova, M. V.; Egorova, O. V. *Appl. Microbiol. Biotechnol.* **2012**, *94*, 1423–1447.
- (6) Crystal data deposited in the Cambridge Crystallographic Data Centre with the deposition number CCDC 985878.
- (7) Weete, J. D. *Phytochemistry* **1973**, *12*, 1843–1864.
- (8) Wang, F.; Fang, Y.; Zhang, M.; Lin, A.; Zhu, T.; Gu, Q.; Zhu, W. *Steroids* **2008**, *73*, 19–26.
- (9) Casiraghi, G.; Zanardi, F.; Appendino, G.; Rassu, G. *Chem. Rev.* **2000**, *100*, 1929–1972.
- (10) Casiraghi, G.; Battistini, L.; Curti, C.; Rassu, G.; Zanardi, F. *Chem. Rev.* **2011**, *111*, 3076–3154.
- (11) Nashed, N. T.; Michaud, D. P.; Levin, W.; Jerina, D. M. *Arch. Biochem. Biophys.* **1985**, *241*, 149–162.
- (12) Keyzers, R. A.; Northcote, P. T.; Webb, V. J. *Nat. Prod.* **2002**, *65*, 598–600.
- (13) Keyzers, R. A.; Northcote, P. T.; Berridge, M. V. *Aust. J. Chem.* **2003**, *56*, 279–282.
- (14) Shi, J.-F.; Wu, P.; Jiang, Z.-H.; Wei, X.-Y. *Eur. J. Med. Chem.* **2014**, *71*, 219–228.
- (15) Wu, P.; Wu, M.; Xu, L.; Xie, H.; Wei, X. *Food Chem.* **2014**, *152*, 23–28.